



Cite this: *Nanoscale*, 2016, **8**, 7840

Received 3rd February 2016,  
 Accepted 10th March 2016

DOI: 10.1039/c6nr01016d

[www.rsc.org/nanoscale](http://www.rsc.org/nanoscale)

## Hollow mesoporous raspberry-like colloids with removable caps as photoresponsive nanocontainers†

Chi Hu,<sup>a</sup> Kevin R. West<sup>b</sup> and Oren A. Scherman<sup>\*a</sup>

**The fabrication, characterisation and controlled cargo release of hollow mesoporous raspberry-like colloids (HMRCs), which are assembled by utilising host–guest complexation of cucurbit[8]uril (CB[8]) are described. CB[8] is employed as a supramolecular linker to ‘stick’ the viologen functionalised paramagnetic iron oxide nanoparticles onto an azobenzene functionalised hollow mesoporous silica core. The formed HMRCs are photoresponsive and can be reversibly disassembled upon light irradiation, endowing them with an ability to release loaded cargo under photocontrol. While the assembled HMRCs retain cargo inside their cavity, disassembled particles with their iron oxide nanoparticle ‘caps’ removed will release the loaded cargo through the mesoporous shell of the hollow silica colloids. A model system using a boronic acid derivative as the cargo in the HMRCs and Alizarin Red salt as a sensor for the released boronic acid is demonstrated.**

Stimuli-responsive nanocontainers are an important class of nanomaterials on account of their ability to precisely change their physical or chemical properties in response to external triggers and carry out controlled cargo release under specific conditions.<sup>1–3</sup> By retaining reactants or catalysts inside, these miniaturized reaction vessels have great potential for improved control over chemical transformations by protecting reagents from the surrounding environments and by releasing them from the confined nanospace over a prolonged period of time.<sup>4–6</sup> The importance of hierarchical hybrid colloids as powerful platforms for the construction of nanocontainers has been recognized by a wide range of researchers.<sup>7–10</sup> For example, yolk-shell nanostructures with a mesoporous silica shell encapsulating a gold nanoparticle yolk were prepared and used as a nanocontainer by Lu and coworkers.<sup>11</sup> Metal oxide nanoparticles such as ZnO and Fe<sub>3</sub>O<sub>4</sub> are attached to the outer surface of mesoporous silica as gatekeepers to obtain

controlled release of loaded cargo.<sup>12,13</sup> Over the past few years, different approaches for constructing hybrid colloids, which contain both organic and inorganic components and exhibit an hierarchical structure, have been developed. Several methods often utilized include the layer-by-layer assembly, which involves depositing alternating layers of oppositely-charged materials,<sup>14,15</sup> while other approaches exploit covalent interactions such as silane chemistry.<sup>16,17</sup> Both of these routes, however, do not often exhibit any intrinsic light-responsiveness, resulting in the lack of photo-controlled activity in the nanocontainers.<sup>18</sup>

Cucurbit[8]uril (CB[8]) is a macrocyclic host molecule, which can simultaneously encapsulate two guest molecules (first and second guests) inside its cavity, forming a stable heteroternary complex.<sup>19,20</sup> CB[8]-directed supramolecular chemistry has been applied in the preparation of a wide range of dynamic hydrogels,<sup>21</sup> supramolecular polymers,<sup>22–24</sup> microcapsules,<sup>25,26</sup> and orthogonal switches.<sup>27</sup> Recently, the host–guest interaction of CB[8] was employed by our group to assemble photoresponsive hybrid raspberry-like colloids, which contain a larger silica core and a corona of polymeric nanoparticles.<sup>28</sup> However, the potential application of these supramolecular hybrid colloids as nanocontainers remains unexplored to date.<sup>29–31</sup>

Herein, we report a facile route to prepare hollow mesoporous raspberry-like colloids (HMRCs), whereby CB[8] is utilized as a supramolecular linker to assemble functional Fe<sub>3</sub>O<sub>4</sub> nanoparticles onto a hollow silica core as shown in Fig. 1. Moreover, the photoresponsive nature of the heteroternary complex composed of viologen (MV, first guest), azobenzene (Azo, second guest) and CB[8] affords HMRC nanocontainers a light-controlled release profile. For the first time, the nanopores of hollow silica colloids are reversibly capped with Fe<sub>3</sub>O<sub>4</sub> nanoparticles through photoresponsive supramolecular interactions, resulting in control over the permeability of the porous silica shell in a remote manner.

Monodispersed hollow mesoporous silica colloids were readily prepared by coating a mesoporous silica shell on the polystyrene latex template by the sol–gel method with the assistance of hexadecyltrimethylammonium bromide (CTAB)

<sup>a</sup>Melville Laboratory for Polymer Synthesis, Department of Chemistry, University of Cambridge, Cambridge, CB2 1EW, UK. E-mail: oas23@cam.ac.uk;

Fax: +44 (0)1223 334866; Tel: +44 (0)1223 331797

<sup>b</sup>BP Oil UK Ltd, Whitchurch Hill, Pangbourne, Reading, Berkshire RG8 7QR, UK

†Electronic supplementary information (ESI) available. See DOI: 10.1039/C6NR01016D

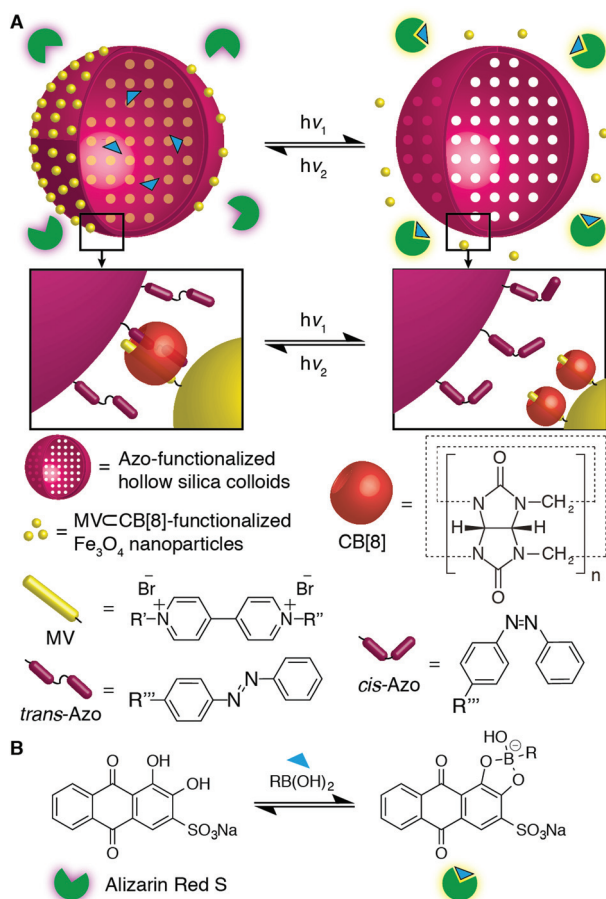


**Fig. 1** Schematic illustration of a light-controlled nanocontainer composed of a hollow silica colloid as the core and  $\text{Fe}_3\text{O}_4$  nanoparticles as coronas. (A) HMRCs obtained through the formation of (MV/trans-Azo)  $\subset$  CB[8] heteroternary complexes and the light-driven reversible disassembly of the HMRCs. (B) A model reaction between boronic acid and Alizarin Red S.

acting as mesopore directing agent and subsequent dissolution of the polystyrene cores.<sup>32–34</sup> Azo-functionalized hollow mesoporous silica colloids (Azo-silica) were prepared by the post-functionalization of the preformed hollow mesoporous silica microspheres using a silane coupling agent with an Azo derivative. The uniform morphology of the Azo-silica colloids is confirmed by the TEM image as shown in Fig. 2A, with a wall thickness of 25 nm. The average diameter ( $D_{\text{TEM}}$ ) and average hydrodynamic diameter ( $D_h$ ) of the Azo-silica core obtained from TEM imaging and dynamic light scattering (DLS) measurements are 330 nm (Fig. 2A) and 435 nm (Fig. 2C), respectively.  $\text{Fe}_3\text{O}_4$  nanoparticles were prepared by Massart's method,<sup>35,36</sup> where two iron salts  $\text{FeCl}_3 \cdot 6\text{H}_2\text{O}$  and  $\text{FeCl}_2 \cdot 4\text{H}_2\text{O}$  were co-precipitated in the presence of  $\text{NH}_4\text{OH}$ . In order to obtain MV-functionalized  $\text{Fe}_3\text{O}_4$  nanoparticles (MV- $\text{Fe}_3\text{O}_4$ ), the preformed  $\text{Fe}_3\text{O}_4$  nanoparticles were functionalized with MV using a silane coupling agent. As shown in Fig. 2B and D, the  $D_{\text{TEM}}$  and  $D_h$  of the MV- $\text{Fe}_3\text{O}_4$  nanoparticles are 7 and 15 nm, respectively.

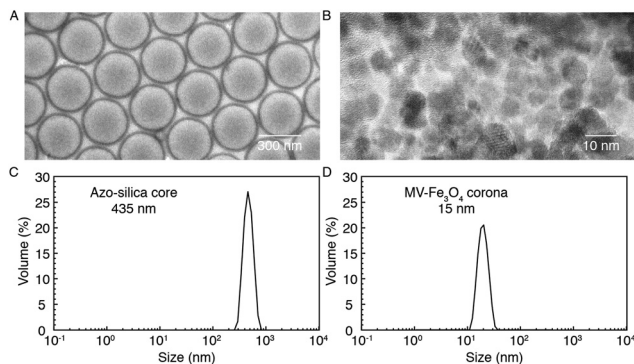


**Fig. 2** Preparation of Azo functionalized hollow mesoporous silica colloids and MV functionalized  $\text{Fe}_3\text{O}_4$  nanoparticles. TEM images of (A) hollow mesoporous Azo-silica colloids and (B) MV- $\text{Fe}_3\text{O}_4$  nanoparticles. DLS results of (C) hollow mesoporous Azo-silica colloids and (D) MV- $\text{Fe}_3\text{O}_4$  nanoparticles.

The HMRCs were then assembled by adding an aqueous dispersion of the Azo-silica colloids into an aqueous dispersion of the MV- $\text{Fe}_3\text{O}_4$  nanoparticles together with CB[8], and sonicated at room temperature for 5 min. As shown in the TEM image in Fig. 3A, well-defined HMRCs with densely packed corona nanoparticles on the surface of the core microsphere can be clearly observed. A zoomed-in image (Fig. 3B) indicates the 25 nm wall of the hollow silica colloids is maintained during the assembly of the raspberry-like structure. The uniform structure of the HMRCs is confirmed by SEM imaging (Fig. 3C), where the measured diameter of the HMRCs corresponds to the  $D_{\text{TEM}}$  of 350 nm as calculated from Fig. 3A and B. It is noteworthy that in order to obtain HMRCs with well-defined structure, the ratio between the Azo-silica colloids and the MV- $\text{Fe}_3\text{O}_4$  nanoparticles is crucial.<sup>28</sup> In order to optimize this ratio, a dispersion of Azo-silica colloids ( $0.3 \text{ g L}^{-1}$ , [Azo] =  $0.01 \text{ mM}$ ) was titrated into a solution of MV- $\text{Fe}_3\text{O}_4$  nano-

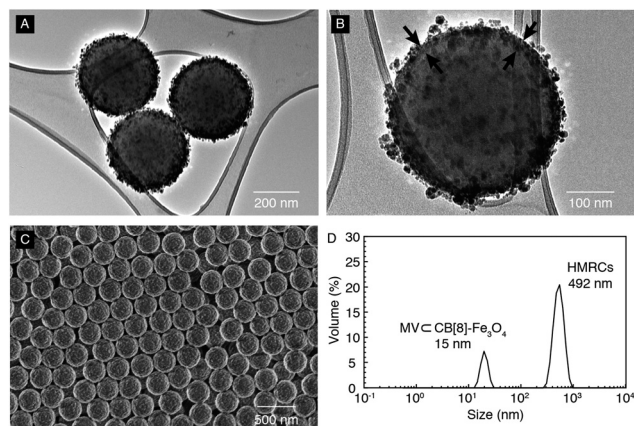


**Fig. 3** Formation of the HMRCs through CB[8]-directed self-assembly. (A) TEM image of the HMRCs. (B) A zoom in image of an HMRC with arrows indicating the shell of the hollow silica colloid. (C) SEM image of the HMRCs cast onto a glass slide. (D) DLS result of the HMRCs formed by the addition of 8 mL Azo-silica colloidal dispersion into 1 mL MV- $\text{Fe}_3\text{O}_4$  nanoparticles/CB[8].

particles (1 mL,  $0.6 \text{ g L}^{-1}$ ,  $[\text{MV}] = 0.01 \text{ mM}$ ) together with CB[8] (0.1 mM), and the assembly process was followed by DLS. Upon the addition of Azo-silica colloids, a new peak at 492 nm was observed, which corresponds to the formation of the HMRCs, while the peak at 15 nm represents the presence of free MV  $\subset$  CB[8]- $\text{Fe}_3\text{O}_4$  nanoparticles (Fig. 3D).

The reversible formation of the HMRCs is readily controlled by UV light irradiation when Azo is employed as the second guest for CB[8]. While *trans*-Azo can be encapsulated into the cavity of CB[8] together with MV to form a heteroternary complex of (MV/*trans*-Azo)  $\subset$  CB[8], *cis*-Azo is not capable of such supramolecular complexation on account of its size.<sup>37–39</sup> As a result, the formed HMRCs disassemble under UV light irradiation (350 nm, 10 min), which transforms *trans*-Azo to *cis*-Azo, disrupting the supramolecular linkage between the Azo-silica spheres and the MV- $\text{Fe}_3\text{O}_4$  nanoparticles (Fig. 4A). This light-triggered disassembly of the HMRCs was also confirmed by DLS (Fig. 4C), where the peak for the HMRCs at 492 nm disappeared while the peak for the Azo-silica colloids at 435 nm was observed together with an increase in the peak intensity at 15 nm for the MV  $\subset$  CB[8]- $\text{Fe}_3\text{O}_4$  nanoparticles. As the Azo-silica colloids and the MV- $\text{Fe}_3\text{O}_4$  nanoparticles were not bonded together at this time, the Azo-silica colloidal solution showed no response to an external magnetic field ( $\vec{B}$ ), thus exhibiting a cloudy appearance, whereas the paramagnetic MV- $\text{Fe}_3\text{O}_4$  nanoparticles organized themselves in the direction of the field (see inset image in Fig. 4C).

This disassembly process can be readily reversed upon exposure to visible light (420 nm, 10 min), which results in the *cis* to *trans* isomerization of Azo derivatives and the simultaneous reassembly of the HMRCs as displayed in the TEM image in Fig. 4B. DLS measurement (Fig. 4D) showed two peaks centered at 15 and 492 nm, which represent the size of the excess free MV  $\subset$  CB[8]- $\text{Fe}_3\text{O}_4$  nanoparticles remaining in the solution and the size of the reassembled HMRCs, respectively. No peak was observed at 435 nm for the free Azo-silica

spheres, indicating the successful reformation of the HMRCs. As all the Azo-silica colloids were bonded together with MV- $\text{Fe}_3\text{O}_4$  nanoparticles through host-guest interactions of CB[8], the dispersion of the reassembled HMRCs exhibited a response to an external magnetic field with all the particles orienting themselves in the direction of the field, leaving behind a clear solution (see inset image in Fig. 4D).

Porous hollow silica spheres have been explored as nanocontainers, but their poor dispersity in aqueous solution and lack of responsivity retard their application. In order to obtain control over the permeability of the porous shell of the hollow silica colloids as well as improve their dispersity in water, here MV- $\text{Fe}_3\text{O}_4$  nanoparticles are utilized to decorate the periphery of hollow silica spheres. Due to the presence of the densely packed nanoparticles, which behave as ‘caps’, the nanochannels of the mesoporous hollow silica colloids become blocked in the HMRCs, resulting in a substantially lower permeability of the nanocontainer. On the other hand, the disassembly of the HMRCs under UV light irradiation ‘opens the nanochannels’ by removing the nanoparticles caps away from the porous hollow silica colloids, thus increasing the permeability of the nanocontainer. The reversible assembly of the HMRCs upon exposure to different light stimuli makes them useful as photo-responsive nanocontainers with controllable permeability.

Alizarin Red salt (AR) displays a dramatic change in fluorescence color and intensity in response to complexation with a boronic acid and can be employed as a general reporter for studying the concentration of boronic acid in solution, both quantitatively and qualitatively.<sup>40</sup> Here the reaction between 3-aminophenylboronic acid (BA) and AR is used to study the light-controlled release profile of the HMRC nanocontainers, as shown in Fig. 1B. In order to load BA molecules inside the cavity of the HMRCs, mesoporous hollow silica colloids were immersed in an aqueous solution of BA (10 mM) for 3 h and collected by centrifuge before assembly with MV  $\subset$  CB[8]- $\text{Fe}_3\text{O}_4$  nanoparticles. The BA-loaded HMRCs were incubated in a solution of AR ( $7 \times 10^{-5} \text{ M}$ , pH adjusted to 7.4 with NaOH) for 20 min, and the UV-vis spectrum of the solution was measured after the removal of the HMRCs by centrifuge as shown in Fig. 5A (cycle 0). In order to control the release of the loaded BA molecules, the dispersion of the BA-loaded HMRCs was exposed to UV light (350 nm) for 10 min to disassemble the raspberry-like structure and ‘open up’ the nanochannels. The UV-vis spectrum was not recorded at this point, as the system with the nanochannels being open was not stable with a large amount of noise. Subsequently, the HMRCs were irradiated with visible light (420 nm) for 10 min to reassemble the raspberry-like structure and ‘close’ the nanochannels, halting the release of BA molecules. The UV-vis spectrum was recorded at this point (cycle 1, Fig. 5A), as well as after incubating the HMRC solution in the dark for 20 min. The spectrum taken after the incubation in the dark is not shown as it did not change at all compared to the spectrum obtained prior to incubation. Alternating UV/visible light irradiation cycles were repeated 10 times, and the UV-vis spectra were recorded after each cycle as shown in Fig. 5A.

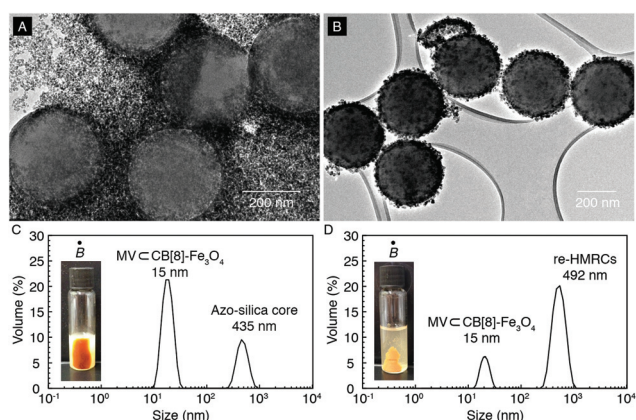


**Fig. 4** The light-driven reversible assembly of the HMRCs. TEM images of (A) the disassembled HMRCs and (B) reassembled HMRCs. DLS results of (C) the disassembled HMRCs and (D) reassembled HMRCs. The inset photos show the magnetic response of the suspensions of disassembled HMRCs and reassembled HMRCs.

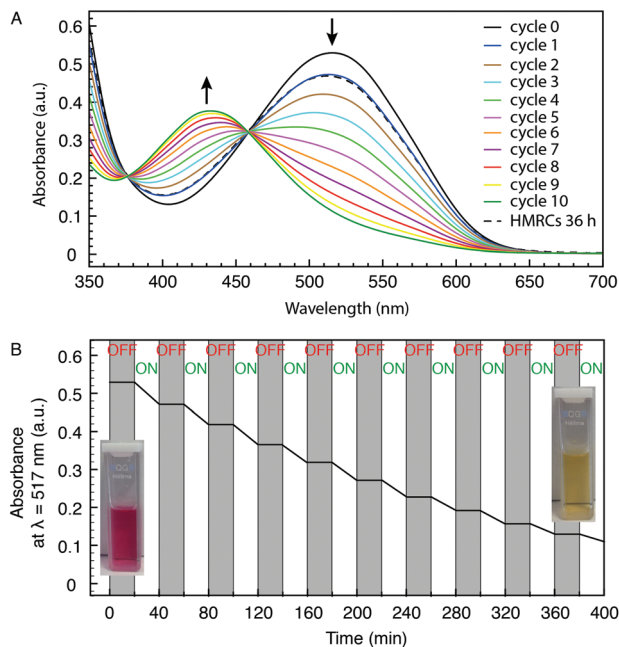


**Fig. 5** Controllable permeability of the HMRCs induced by light irradiation. (A) UV-vis traces of the AR solution (pH = 7.4) after different cycles of the light-triggered release of BA. The dashed line shows the UV-vis spectrum of the AR solution with the HMRCs immersed in for 36 h. Measurements were recorded after the removal of HMRCs. (B) Kinetic plot of the BA release during UV and visible light irradiation for 10 cycles. The inset images show the color change of the AR solution before and after the release of BA from the HMRCs. Images were taken after the removal of HMRCs.

Before complexing with BA, AR showed an absorbance peak at 517 nm in its UV-vis spectrum and exhibited a pink color. As AR started to complex with the BA molecules in solution that were released from the HMRC nanocontainers, AR exhibited a color change, from pink to yellow (see inset images in Fig. 5B), with a decrease in absorbance at 517 nm. Meanwhile, a new peak for the AR/BA complex centered at 432 nm was observed together with an isosbestic point at 461 nm, indicating that the AR and AR/BA complex are related linearly by stoichiometry.

In order to study the release kinetics of BA molecules from the HMRC nanocontainers, the absorbance of the AR solution at 517 nm was plotted against irradiation time as shown in Fig. 5B. An on-off release profile, which is controlled by alternating UV/visible light irradiation, can clearly be observed. While the absorbance did not exhibit any decay during the 20 min time intervals of incubation in the dark (OFF), it decreased upon irradiation with UV/visible light (ON) with a reduced gradient with the revolution of time, suggesting the AR/BA complexation is approaching its equilibrium.

In conclusion, hollow mesoporous raspberry-like colloids (HMRCs) bearing hollow silica microspheres as the core and paramagnetic  $\text{Fe}_3\text{O}_4$  nanoparticles as the corona have been prepared by utilizing host-guest complexation of CB[8] at their interface. CB[8] was employed as supramolecular 'glue' to

'stick' together the viologen (MV) functionalized  $\text{Fe}_3\text{O}_4$  nanoparticles and the azobenzene (Azo) functionalized hollow silica colloids by forming a heteroternary complex of (MV/*trans*-Azo)  $\subset$  CB[8]. Moreover, the formation of this raspberry-like structure is reversible upon UV light irradiation, resulting in the *trans* to *cis* isomerization of Azo derivatives and the dissociation of the heteroternary complex. Most importantly, the HMRCs can be used as nanocontainers with a light-controllable permeability. While the nanochannels of the assembled HMRCs are 'capped' with the  $\text{Fe}_3\text{O}_4$  nanoparticles, they can be 'opened' by removing the  $\text{Fe}_3\text{O}_4$  nanoparticles under UV irradiation, resulting in the release of the loaded cargo. A model system using boronic acid (BA) as the cargo in the HMRCs and Alizarin Red salt as a sensor for the BA is shown here, suggesting a general application of the HMRCs as photo-responsive nanocontainers.

## Acknowledgements

This work was supported by the Engineering Physical Science Research Council, grant EP/K028510/1. C. Hu thanks BP for financial support and Hughes Hall College Cambridge for a student scholarship.

## References

- 1 F. Meng, Z. Zhong and J. Feijen, *Biomacromolecules*, 2009, **10**, 197–209.
- 2 S. Mura, J. Nicolas and P. Couvreur, *Nat. Mater.*, 2013, **12**, 991–1003.
- 3 S. Ganta, H. Devalapally, A. Shahiwala and M. Amiji, *J. Controlled Release*, 2008, **126**, 187–204.
- 4 L. K. Yeung and R. M. Crooks, *Nano Lett.*, 2001, **1**, 14–17.
- 5 M. L. Zheludkevich, D. G. Shchukin, K. A. Yasakau, H. Möhwald and M. G. S. Ferreira, *Chem. Mater.*, 2007, **19**, 402–411.
- 6 J. A. Hubbell and A. Chilkoti, *Science*, 2012, **337**, 303–305.
- 7 J. Lee, J. C. Park and H. Song, *Adv. Mater.*, 2008, **20**, 1523–1528.
- 8 Z. Chen, Z.-M. Cui, F. Niu, L. Jiang and W.-G. Song, *Chem. Commun.*, 2010, **46**, 6524–6526.
- 9 G. Ruan, G. Vieira, T. Henighan, A. Chen, D. Thakur, R. Sooryakumar and J. O. Winter, *Nano Lett.*, 2010, **10**, 2220–2224.
- 10 R. Liu, X. Zhao, T. Wu and P. Feng, *J. Am. Chem. Soc.*, 2008, **130**, 14418–14419.
- 11 J. Liu, S. Qiao, S. Budi Hartono and G. Lu, *Angew. Chem., Int. Ed.*, 2010, **49**, 4981–4985.
- 12 S. Wu, X. Huang and X. Du, *J. Mater. Chem. B*, 2015, **3**, 1426–1432.
- 13 S. Giri, B. G. Trewyn, M. P. Stellmaker and V. S.-Y. Lin, *Angew. Chem., Int. Ed.*, 2005, **44**, 5038–5044.
- 14 F. Caruso, R. A. Caruso and H. Möhwald, *Science*, 1998, **282**, 1111–1114.

- 15 D. Shchukin, M. Zheludkevich, K. Yasakau, S. Lamaka, M. Ferreira and H. Möhwald, *Adv. Mater.*, 2006, **18**, 1672–1678.
- 16 S. Wu, J. Dzubielia, J. Kaiser, M. Drechsler, X. Guo, M. Ballauff and Y. Lu, *Angew. Chem., Int. Ed.*, 2012, **51**, 2229–2233.
- 17 A. Guerrero-Martínez, J. Pérez-Juste and L. M. Liz-Marzán, *Adv. Mater.*, 2010, **22**, 1182–1195.
- 18 M.-L. Guan, D.-K. Ma, S.-W. Hu, Y.-J. Chen and S.-M. Huang, *Inorg. Chem.*, 2011, **50**, 800–805.
- 19 J. W. Lee, S. Samal, N. Selvapalam, H.-J. Kim and K. Kim, *Acc. Chem. Res.*, 2003, **36**, 621–630.
- 20 F. Biedermann, V. D. Uzunova, O. A. Scherman, W. M. Nau and A. De Simone, *J. Am. Chem. Soc.*, 2012, **134**, 15318–15323.
- 21 E. A. Appel, F. Biedermann, U. Rauwald, S. T. Jones, J. M. Zayed and O. A. Scherman, *J. Am. Chem. Soc.*, 2010, **132**, 14251–14260.
- 22 Y. Liu, H. Yang, Z. Wang and X. Zhang, *Chem. – Asian J.*, 2013, **8**, 1626–1632.
- 23 Y. Liu, Y. Yu, J. Gao, Z. Wang and X. Zhang, *Angew. Chem., Int. Ed.*, 2010, **49**, 6576–6579.
- 24 S. Dong, B. Zheng, F. Wang and F. Huang, *Acc. Chem. Res.*, 2014, **47**, 1982–1994.
- 25 J. Zhang, R. J. Coulston, S. T. Jones, J. Geng, O. A. Scherman and C. Abell, *Science*, 2012, **335**, 690–694.
- 26 Y. Zheng, Z. Yu, R. M. Parker, Y. Wu, C. Abell and O. A. Scherman, *Nat. Commun.*, 2014, **5**, 5772.
- 27 F. Tian, D. Jiao, F. Biedermann and O. A. Scherman, *Nat. Commun.*, 2012, **3**, 1207.
- 28 Y. Lan, Y. Wu, A. Karas and O. A. Scherman, *Angew. Chem., Int. Ed.*, 2014, **53**, 2166–2169.
- 29 C. Park, H. Kim, S. Kim and C. Kim, *J. Am. Chem. Soc.*, 2009, **131**, 16614–16615.
- 30 K. Patel, S. Angelos, W. R. Dichtel, A. Coskun, Y.-W. Yang, J. I. Zink and J. F. Stoddart, *J. Am. Chem. Soc.*, 2008, **130**, 2382–2383.
- 31 C.-L. Zhu, C.-H. Lu, X.-Y. Song, H.-H. Yang and X.-R. Wang, *J. Am. Chem. Soc.*, 2011, **133**, 1278–1281.
- 32 G. Qi, Y. Wang, L. Estevez, X. Duan, N. Anako, A.-H. A. Park, W. Li, C. W. Jones and E. P. Giannelis, *Energy Environ. Sci.*, 2011, **4**, 444–452.
- 33 H. Bamnolker, B. Nitzan, S. Gura and S. Margel, *J. Mater. Sci. Lett.*, 1997, **16**, 1412–1415.
- 34 Z. Deng, M. Chen, S. Zhou, B. You and L. Wu, *Langmuir*, 2006, **22**, 6403–6407.
- 35 R. Massart, *IEEE Trans. Magn.*, 1981, **17**, 1247–1248.
- 36 J. Liu, C. Detrembleur, A. Debuigne, M.-C. De Pauw-Gillet, S. Mornet, L. Vander Elst, S. Laurent, C. Labrugere, E. Duguet and C. Jerome, *Nanoscale*, 2013, **5**, 11464–11477.
- 37 C. Stoffelen, J. Voskuhl, P. Jonkheijm and J. Huskens, *Angew. Chem., Int. Ed.*, 2014, **53**, 3400–3404.
- 38 H.-B. Cheng, Y.-M. Zhang, C. Xu and Y. Liu, *Sci. Rep.*, 2014, **4**, 4210.
- 39 J. del Barrio, P. N. Horton, D. Lairez, G. O. Lloyd, C. Toprakcioglu and O. A. Scherman, *J. Am. Chem. Soc.*, 2013, **135**, 11760–11763.
- 40 G. Springsteen and B. Wang, *Chem. Commun.*, 2001, 1608–1609.